Photoaffinity labeling of chloroplast cytochrome b_6–f complex by an inhibitor azido-derivative

Walter Oettmeier, Klaus Masson and Ellen Olschewski

Lehrstuhl Biochemie der Pflanzen, Ruhr-Universität, Postfach 10 21 48, 4630 Bochum 1, FRG

Received 21 March 1983

The photoaffinity label 2-azido-2′,4,4′-trinitro-6-*sec.*butyldiphenylether inhibits photosynthetic electron transport in the thylakoid membrane as well as plastohydroquinone–plastocyanin-oxidoreductase activity in the isolated chloroplast cytochrome b_6–f complex. In the latter, the ^{14}C-labeled inhibitor upon UV-irradiation binds covalently only to the cytochrome b_6 and the Rieske Fe–S peptide subunit.

Photoaffinity label *Cytochrome* b_6–f *complex* *Inhibitor* *Plastoquinone* *Rieske Fe–S protein* *Cytochrome* b_6

1. INTRODUCTION

Photoaffinity labels are useful tools for identification of binding sites for substrates and inhibitors on enzymes and membrane-bound proteins. In respiratory and photosynthetic electron transport, the binding domains for ubiquinone or plastoquinone could be identified using quinone-derived photoaffinity labels [1,2]. Upon light activation in chloroplast cytochrome b_6–f complex, a plastoquinone-azide exclusively labels the cytochrome b_6 and the Rieske Fe–S protein [2] out of 5 polypeptides (33, 34 kDa, cytochrome f; 23.5 kDa, cytochrome b_6; 20 kDa, Rieske Fe–S protein; 17.5 kDa, function not known yet) [3,4].

Here we report that an azido-analogue of the inhibitor 2-iodo-2′,4,4′-trinitro-3-methyl-6-isopropyl–diphenylether (DNP-INT), which is suggested to prevent plastohydroquinone oxidation by interaction with the cytochrome b_6–f complex [5,6] exhibits an identical labeling pattern like plastoquinone azide. This further supports the idea that two different electron carriers (the cytochrome b_6 and the Rieske Fe–S protein) take part in plastohydroquinone oxidation.

2. MATERIALS AND METHODS

2.1. *2-Azido-4-nitro-6-*sec.*butylphenol synthesis*

To 1.05 g (5 mmol) 2-amino-4-nitro-6-*sec.*butylphenol [7] in 20 ml, 35% fluoroboric acid was slowly added under stirring a solution of 0.69 g (10 mmol) $NaNO_2$ in 4 ml H_2O. The temperature was maintained at 5°C. After 15 min stirring, excess $NaNO_2$ was destroyed by addition of 0.6 g (10 mmol) urea in 3 ml H_2O. Then a solution of 0.65 g (10 mmol) NaN_3 in 5 ml H_2O was added. The reaction mixture was stirred at 0°C for 15 h and then extracted 3 times with ether. The ether phase was dried over $MgSO_4$, the ether evaporated in the vacuum and the residue chromatographed on silica gel (3.5 × 30 cm) with benzene as the solvent. Recrystallized from CCl_4/petrol ether, yield 0.51 g (43%); m.p. 82–83°C (dec.). Calc. %: C, 50.84; H, 5.12; N, 23.72. Found %: C, 50.68; H, 5.16; N, 23.5.

2.2. *2-Azido-2′,4,4′-trinitro-6-*sec.*butyldiphenylether (DNP-ANT) synthesis*

A mixture of 118 mg (0.5 mmol) 2-azido-4-nitro-6-*sec.*butylphenol, 74.4 mg (0.4 mmol) 2,4-dinitrofluorobenzene and 34 mg (0.1 mmol) tetrabutylammonium hydrogen sulfate in 15 ml

Published by Elsevier Science Publishers B.V.
00145793/83/$3.00

CH_2Cl_2, 14 ml H_2O and 1 ml 1 N NaOH was stirred for 24 h at room temperature. The CH_2Cl_2 was allowed to evaporate during the reaction. The precipitate was dissolved in ether and extracted 2 times with 0.01 N NaOH. The ether phase was dried with $MgSO_4$ and the ether evaporated in the vacuum. Recrystallized from ethyl acetate/petrol ether, yield 42.8 mg (27%); m.p. 98°C. Calc. %: C, 47.76; H, 3.51; N, 20.89. Found %: C, 46.85; H, 3.79; N, 20.5. UV/vis (methanol): 252 (ϵ = 19 580 $M^{-1}.cm^{-1}$), 280 nm.

2.3. *2-Azido-2',4,4'-trinitro-6-*sec.*butyl-di[U-^{14}C]phenylether ([^{14}C]DNP-ANT) synthesis*

A mixture of 2.26 mg (9.6 μmol) 2-azido-4-nitro-6-*sec.*butylphenol, 0.885 mg (4.8 μmol) 2,4-dinitrofluoro-[U-^{14}C]benzene (100 μCi; Amersham/Buchler, Braunschweig), 1 mg tetrabutylammonium hydrogen sulfate, and 9.6 μl 1 N NaOH in 0.5 ml H_2O and 0.5 ml CH_2Cl_2 was stirred at room temperature. The CH_2Cl_2 was allowed to evaporate and replaced 3 times. After 5 h the reaction mixture was extracted 3 times with ether, the ether phase dried over $MgSO_4$ and the ether solution concentrated in the vacuum. Aliquots of ~70 μl were chromatographed on silica gel-precoated plastic sheets 60 F-254 (Merck AG, Darmstadt) with petrol ether (boiling range 40–60°C)/ethyl acetate (85/15, v/v) as the eluent. The zone corresponding to [^{14}C]DNP-ANT (R_F 0.77) was cut out and eluted with methanol. The concentration of [^{14}C]DNP-ANT was determined from the absorption at 252 nm. The compound was obtained in a yield of 42% and spec. act. 14.4 mCi/mmol.

2.4. *2,3-Dimethyl-5-(4'-acetoxy-*n*-butyl)-1,4-benzohydroquinone (DABH) synthesis*

2.08 g (10 mmol) 2,3-dimethyl-5-(4'-hydroxy-*n*-butyl)-1,4-benzoquinone [2] in 100 ml abs. THF, 1.4 ml (16.2 mmol) acetyl chloride and 1.3 ml pyridine were stirred at room temperature for 3 h. Then THF was evaporated in the vacuum, the residue taken up in 250 ml ether and extracted several times with 0.01 N HCl. The ether phase after drying over $MgSO_4$ was evaporated in the vacuum. The crystalline residue was dissolved in 50 ml methanol and hydrogenated catalytically with 0.2 g Pd/C as the catalyst. Recrystallized from benzene/petrol ether, yield 1.60 g (64%), m.p. 73°C. Calc. %: C, 66.64; H, 7.99. Found %: C, 66.67; H, 8.04.

2.5. *Biochemical methods*

Chloroplasts from spinach were prepared as in [8] and cytochrome b_6–f complex as in [4]. Chloroplasts were stored in liquid nitrogen in the presence of 10% glycerol.

Photosynthetic electron transport from H_2O to ferricyanide was measured spectroscopically at 420 nm in a Zeiss PMQII spectrophotometer modified for cross illumination with red light (filter, Schott RG 630; light intensity, 0.1 $W.cm^{-2}$). The reaction mixture contained in 2 ml: 40 mM Tricine (pH 8.0); 10 mM $MgCl_2$; 1 mM ferricyanide; 7 μg gramicidine. The control rate was 256 μmol ferricyanide reduced.mg $chl^{-1}.h^{-1}$.

Plastohydroquinone–plastocyanin-oxidoreductase activity was determined by following plastocyanin reduction spectroscopically at 597–500 nm in an Aminco DW-2 spectrophotometer. The reaction mixture contained 1 ml: 30 mM MES (pH 6.5); 3.8 μM plastocyanine, 0.1 mM DABH, and 56.9 nM cytochrome b_6–f complex.

For the labeling experiments, aliquots of the cytochrome b_6–f complex (corresponding to 800 pmol cytochrome f) in 40 μl 30 mM octylglycoside, 0.5% cholate, and 30 mM Tris/succinate buffer (pH 6.5) together with DNP-ANT were UV-irradiated (Zeiss mercury lamp Qu2) in small quartz vials under cooling and in a nitrogen atmosphere for 10 min. Solubilization, polyacrylamide gel electrophoresis, and assay for radioactivity were performed as in [9], except that Li-dodecylsulfate was used instead of Na-dodecylsulfate and gels were run at 4°C.

3. RESULTS AND DISCUSSION

DNP-INT (fig.1) has been introduced as an inhibitor of photosynthetic electron transport, which in its mode of action is similar to 2,5-dibromo-3-methyl-6-isopropyl–1,4-benzoquinone (DBMIB). It supposedly blocks plastohydroquinone oxidation, but unlike DBMIB does not exhibit redox properties [5,6]. The synthesis of the photoaffinity label analogue DNP-ANT (fig.1) of this inhibitor started from the well known her-

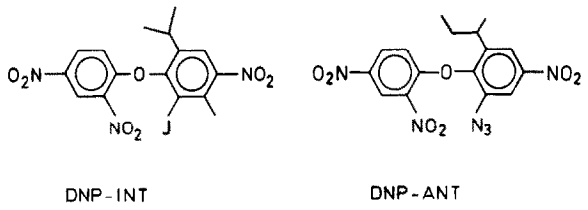

Fig.1. Chemical structures of inhibitors DNP-INT and DNP-ANT.

bicide 2,4-dinitro-*sec.*butylphenol (dinoseb), which by selective reduction, diazotation, and reaction with NaN_3 could be converted to 2-azido-4-nitro-6-*sec.*butylphenol. This azide, by reaction with 2,4-dinitro-fluoro-[U-^{14}C]benzene yielded DNP-ANT. The alkyl substitution pattern of DNP-ANT is slightly different from DNP-INT (*sec.*butyl instead of methyl, isopropyl), but as has been demonstrated for the series of corresponding phenolic inhibitors, different alkyl-substituted phenols do not differ substantially in their inhibitory activity, provided the alkyl substituent is bulky enough [10].

The inhibitor properties of DNP-ANT on uncoupled photosynthetic electron flow from water to ferricyanide in comparison with DNP-INT are demonstrated in fig.2. As usually inhibitory activity is strictly dependent on [chl]. The I_{50}-value (i.e., concentration necessary for 50% inhibition) decreases with decreasing [chl]. In general, DNP-ANT is less inhibitory than DNP-INT. This result is not unexpected, because in the corresponding phenol series, activity decreases in the order I > Br > Cl [10]. The same is true for inhibitory activity of halogenated quinones [11]. It is known that the azido group in its chemical properties closely resembles Cl. Differences in I_{50}-values for both compounds become less pronounced with decreasing [chl] and the following I_{50}-values, extrapolated to zero [chl] can be obtained: DNP-INT, 1.2×10^{-7} M; DNP-ANT, 1.5×10^{-7} M.

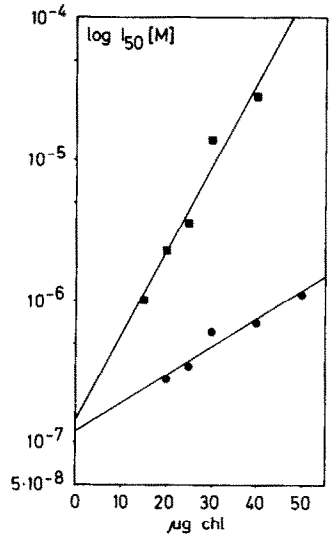

Fig.2. Dependence from chl concentration of I_{50}-values for DNP-INT (■—■) and DNP-ANT (●—●). Photosynthetic electron transport from H_2O to ferricyanide was measured as in section 2. I_{50}-values were interpolated graphically from electron-transport rates at different inhibitor concentrations.

DNP-ANT is also an efficient inhibitor of plastohydroquinone–plastocyanin-oxidoreductase activity of isolated chloroplast cytochrome b_6–f complex (fig.3). In this system, DABH has been used as the donor instead of plastohydroquinone-1. Although DABH is less effective as donor as compared to plastohydroquinone-1, it has the advantage of being less autoxidizable than the latter compound. DNP-ANT like in the chloroplast system is less inhibitory active than DNP-INT (fig.3).

The labeling pattern of chloroplast cytochrome b_6–f complex by different concentrations of [^{14}C]DNP-ANT is demonstrated in fig.4. Radioactivity is almost exclusively found in two polypeptides: the cytochrome b_6 (23.5 kDa) and the Rieske Fe–S protein (20 kDa).

The radioactivity found at the front of the gel

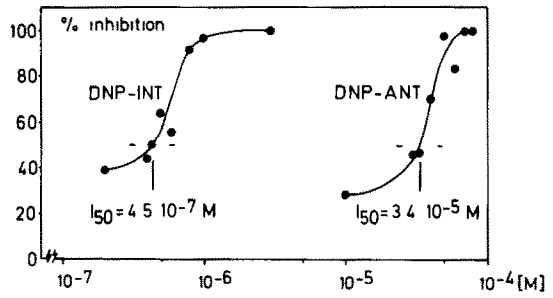

Fig.3. Inhibition of plastohydroquinone–plastocyanin-oxidoreductase activity of isolated chloroplast cytochrome b_6–f complex by DNP-INT and DNP-ANT: Donor, DABH; acceptor, plastocyanin; for conditions see section 2. The control rate was 68 µmol plastocyanin reduced/h.

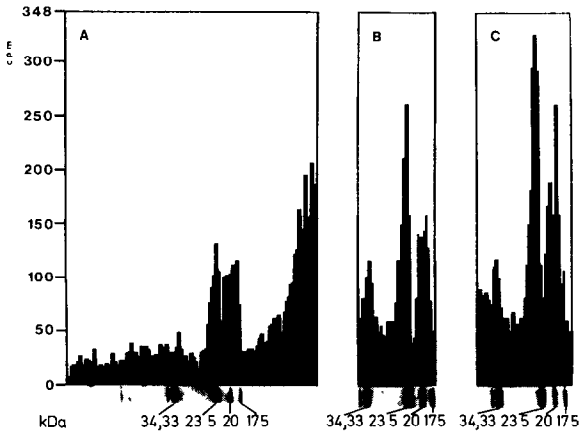

Fig.4. Photographs of polyacrylamide gels of chloroplast cytochrome b_6–f complex and radioactivity distribution after labelling at different amounts of [^{14}C]DNP-ANT (A, 2.4; B, 4.8; C, 9.6 nmol). The bars in the histogram correspond to the radioactivity count in 1 mm gel pieces. The amount of the complex was the same in all experiments and corresponded to 0.8 nmol cytochrome f. In (A) the whole gel and in (B,C) only the relevant parts are shown.

(fig.4A, right) is due to low-M_r labeled compounds and decomposition products of DNP-ANT after UV-irradiation. Even at the highest concentration of [^{14}C]DNP-ANT applied, the amount of labeling in the cytochrome f (33, 34 kDa) and the 17.5 kDa subunit is very small (fig.3C). Furthermore, incubation of cytochrome b_6–f complex with DNP-INT or DBMIB prior to addition of [^{14}C]DNP-ANT and UV-irradiation diminishes the amount of labeling in the cytochrome b_6 and the Rieske Fe–S protein considerably (not shown). Due to the small residual radioactivity in these samples we cannot decide whether there is preferential binding of DNP-ANT to the cytochrome b_6 or Rieske Fe–S protein in the presence of these inhibitors.

The labeling pattern of chloroplast cytochrome b_6–f complex is very similar to that obtained with [^{3}H]plastoquinone-azide [2]. This result is important for three reasons:

(1) It eliminates some doubts concerning the labeling specificity of the plastoquinone-azide which have been raised due to the fact that the azido function in the plastoquinone-azide is some 10 Å apart from the quinone moiety. This could have led to labeling of an adjacent protein not directly involved in plastohydroquinone oxidation. Since an identical labeling pattern is obtained by [^{14}C]DNP-ANT where the azido function is in the very middle of a comparatively small molecule, this possibility can be excluded.

(2) It indicates that the native donor plastohydroquinone and the inhibitors DNP-ANT or DNP-INT, respectively, bind to the same subunits of the complex, and consequently, DNP-INT and DNP-ANT indeed block plastohydroquinone oxidation.

(3) It further strengthens the idea of a two step oxidation of plastohydroquinone via the semiquinone and a 'Q- or b-cycle' mechanism, where two different redox couples (plastohydroquinone/plastosemiquinone and plastosemiquinone/plastoquinone) funnel electrons into two different redox carriers (cytochrome b_6 and Rieske Fe–S protein) [12,13].

ACKNOWLEDGEMENTS

This work was supported by Deutsche Forschungsgemeinschaft. We are indebted to Professor Dr A. Trebst for many helpful discussions.

REFERENCES

[1] Yu, C.A. and Yu, L. (1980) Biochem. Biophys. Res. Commun. 96, 286–292.
[2] Oettmeier, W., Masson, K., Soll, H.J., Hurt, E. and Hauska, G. (1982) FEBS Lett. 144, 313–317.
[3] Hurt, E. and Hauska, G. (1981) Eur. J. Biochem. 117, 591–599.
[4] Hurt, E. and Hauska, G. (1982) J. Bioenerg. Biomembr. 14, 405–424.
[5] Trebst, A., Wietoska, H., Draber, W. and Knops, H.J. (1978) Z. Naturforsch. 33c, 919–927.
[6] Draber, W., Knops, H.J. and Trebst, A. (1981) Z. Naturforsch. 36c, 848–852.
[7] Ernst, W. and Bär, F. (1964) Arzneimittelforsch. 14, 81–84.
[8] Nelson, N., Drechsler, Z. and Neumann, J. (1970) J. Biol. Chem. 245, 143–151.
[9] Oettmeier, W., Masson, K. and Johanningmeier, U. (1980) FEBS Lett. 118, 267–270.
[10] Trebst, A., Reimer, S., Draber, W. and Knops, H.J. (1979) Z. Naturforsch. 34c, 831–840.
[11] Oettmeier, W., Reimer, S. and Link, K. (1978) Z. Naturforsch. 33c, 695–703.
[12] Malkin, R. (1981) FEBS Lett. 131, 169–172.
[13] Selak, M.A. and Whitmarsh, J. (1982) FEBS Lett. 150, 286–292.